Hyperfine structure of the $^1D_2$-$^3H_4$ levels of Pr^{3+}:LaF_3 with the use of photon echo modulation spectroscopy

E. A. Whittaker and S. R. Hartmann
Columbia Radiation Laboratory, Department of Physics, Columbia University, New York, New York 10027
(Received 1 March 1982)

We have performed a photon echo modulation measurement of the $^1D_2$-$^3H_4$ levels of Pr^{3+}:LaF_3. This time-domain method yields a precise determination of the $^1D_2$ excited-state hyperfine splittings and linewidths. New information on the relative orientation of the principal axes of the excited- and ground-state hyperfine Hamiltonians is presented.

In this paper we present the results of a photon echo modulation measurement of the hyperfine structure and line-broadening character of the lowest crystal-field-split levels of the $^1D_2$-$^3H_4$ transition in Pr^{3+}:LaF_3. These electronic singlets are each split into three pairs of doublets by the second-order hyperfine and electric quadrupole interactions.[1,2] The splittings are of the order of 10 MHz. Both the nuclear and the optical transitions of this system are broadened by the magnetic interaction of the Pr and F nuclei.[3] While the nuclear magnetic interactions are enhanced by second-order electronic coupling,[4] these interactions are still weak, and the optical homogeneous linewidth is one of the narrowest ever seen in a solid.[5] The spectra described in this paper have been measured previously by enhanced and saturated absorption,[2] photon echo nuclear double resonance,[6] and nonmodulated photon echo.[5] Our result, however, represents the first measurement of the splittings and linewidths of this transition carried out entirely in the time domain and provides new information on the relative orientation of the principal axes systems of the ground $^3H_4$ and excited $^1D_2$ hyperfine Hamiltonians.

Hyperfine spectroscopy using photon echo modulation has been described completely by Chen *et al.*[7] who studied the $^3P_0$-$^3H_4$ transition in Pr^{3+}:LaF_3. We summarize here the basic method and some improvements we have made. Two laser pulses, resonant with the $^1D_2$-$^3H_4$ transition and separated in time by τ, are incident upon a 10-mm-long sample, cooled to 2.5 K. This preparation gives rise to a rephased dipole moment at time 2τ after the first pulse, given by

$$P(2\tau)=\vec{P}(0)(2I+1)^{-1}\sum_{\alpha,\beta,\gamma,\epsilon=1}^{2I+1}(W)_{\alpha\beta}(W^{-1})_{\beta\gamma}(W)_{\gamma\epsilon}(W^{-1})_{\epsilon\alpha}\exp[-(\Omega^{(e)}_{\alpha\gamma}+\Omega^{(g)}_{\beta\epsilon})\tau]$$
$$\times\cos[(\omega^{(e)}_{\alpha\gamma}-\omega^{(g)}_{\beta\epsilon})\tau]\exp(-2\tau/T_2)\,, \quad (1)$$

where the notation is that of Ref. 7. The essential features of this formula are its dependence on the W matrices, which carry information on the relative orientation of the ground- and excited-state hyperfine Hamiltonians, the nuclear hyperfine transition linewidths Ω, and the nuclear hyperfine transition frequencies ω. The measured echo intensity is the square of this amplitude and will contain beats from both the fundamental hyperfine frequencies and their harmonics.

The experimental method utilizes two electronically triggered nitrogen laser-pumped dye lasers. The 1-GHz wide, kilowatt pulses are made collinear and focused to a 100-μm spot on the 0.1 wt. % sample of Pr^{3+}:LaF_3. The echo signal is detected through a Pockels cell shutter by an RCA C31034 photomultiplier tube. A PDP8/e computer is used to control and sweep the laser pulse separation through a desired range, and to integrate and digitize the echo intensity for each laser shot. To eliminate the effects of a remnant (10–20)-nsec laser pulse separation jitter, a computer-read ORTEC 457 time-to-pulse-height converter is used to put each echo shot into the appropriate 5-nsec-wide bin in the computer memory. To compensate for laser amplitude drift and to facilitate averaging data from many sweeps, the computer was made to periodically record the echo intensity at a fixed

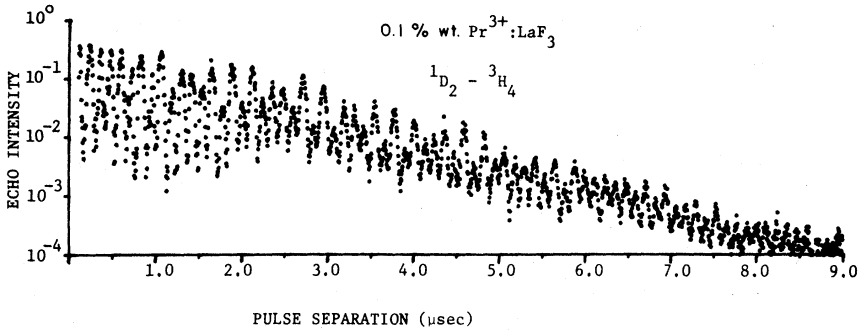

FIG. 1. Photon echo intensity vs laser pulse separation for the $^1D_2$-$^3H_4$ transition of 0.1 wt. % Pr^{3+}:LaF_3.

reference time ($\tau = 600$ nsec). Figure 1 shows the average echo intensity versus pulse separation. Each point is the average of at least 100 shots and the data shown represent the average of about 30 separate runs. A given run covers about 1 μsec of data. To eliminate the effect of optical pumping in the ground state[1] (which for this method produces an artifact known as long-lived stimulated echo[8]), the 16.7-MHz ground-state hyperfine resonance is saturated with rf energy between laser shots.

The overall decay of the echo in Fig. 1 reflects a homogeneous optical linewidth of 72 kHz (corresponding to $T_2 = 4.4$ μsec for a Lorentzian line shape), consistent with several other recent measurements.[5,9] More information may be extracted from this data by examining its Fourier transform, shown in Fig. 2. Before Fourier transformation, the data of Fig. 1 were multiplied by a factor $\exp(+4\tau/T_2)$ so that the resonance linewidths of Fig. 2 do not include the overall optical decay linewidth. The three strong resonances at 3.72, 4.79, and 8.51 MHz are the hyperfine frequencies of the $^1D_2$ excited states. Weaker resonances (note that beyond 10 MHz the vertical scale is 100 times more sensitive) at 12.24, 13.26, and 17.04 MHz are from mixing of the first three strong resonances. There are also ground-state resonances at 8.48, 16.7, and 25.14 MHz but the 8.48-MHz line is masked by the stronger 8.51-MHz excited-state line, and the 16.7-MHz line appears to be split. We believe that this splitting is an unanticipated effect of the 16.7-MHz rf energy used to eliminate long-lived stimulated echo, and probably arises because for pulse separations greater than 3 μsec the rf energy was inadvertently allowed to overlap the echo pulse sequence.

The resonance widths reflect the total (inhomogeneous and homogeneous) nuclear linewidths of the various hyperfine transitions. Previous measurements[1,7] have shown the ground-state widths to be about 200 kHz. This width is mostly inhomogeneous and arises from the interaction of the enhanced ground-state ^{141}Pr nuclear moment of 11.5 kHz/G (Ref. 1) and the surrounding distribution of static ^{19}F nuclear moments. Macfarlane and Shelby[10] have measured the g tensor for the $^1D_2$ state and found the enhancement to be roughly 5 times less than in the ground state. This would lead one to expect a much narrower linewidth for the nuclear transitions in the $^1D_2$ state and our measurement, while very nearly resolution limited by the overall echo-decay envelope, places a new upper limit of 30 kHz (full width at half maximum) for the 8.51-MHz linewidth, consistent with this expectation. The 3.72- and 4.79-MHz linewidths are

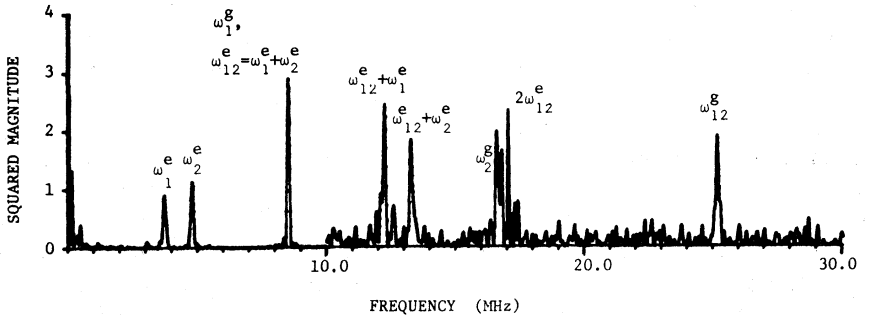

FIG. 2. Squared magnitude of the Fourier transform of the data in Fig. 1. The data were first multiplied by $\exp(\tau/1.2$ μsec). The vertical scale is 100 times more sensitive for frequencies beyond 10 MHz.

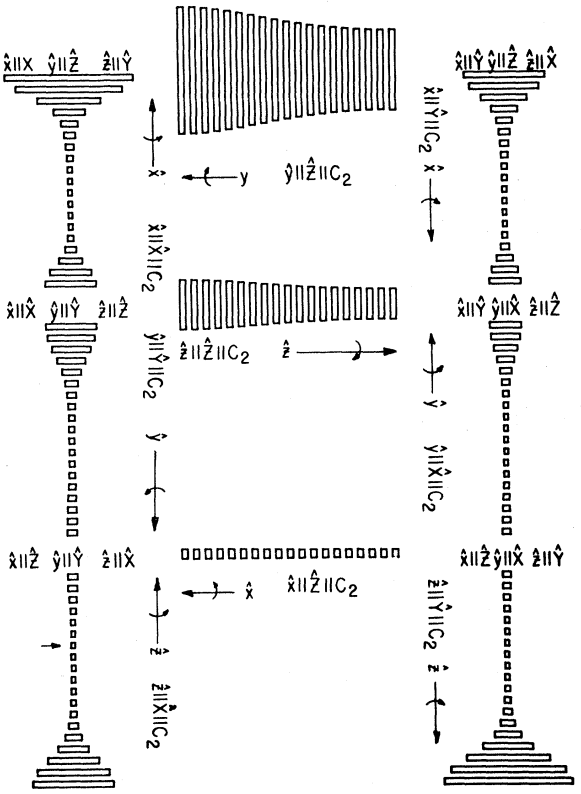

FIG. 3. Map of minimum mean-square deviation between echo data and theoretical curve of Eq. (1), as a function of the relative orientation of the ground- and excited-state hyperfine Hamiltonians. The arrow at the lower left points to the coordinate with the best fit.

somewhat larger, at 70 and 60 kHz, respectively. The results for the $^1D_2$ excited-state parameters are summarized in Table I.

The expression for echo modulation is given analytically by Eq. (1). Once Fourier analysis has given the splittings and linewidths, the only remaining parameters define the relative orientation of the ground- and excited-state effective hyperfine Hamiltonian principal axes. This Hamiltonian may be written

$$H_{g(e)}=P_{g(e)}\left[I^2_{z(Z)}+\frac{\eta_{g(e)}}{3}(I^2_{x(X)}-I^2_{y(Y)})\right]. \tag{2}$$

The upper and lower case subscripts emphasize that the ground (g) and excited (e) state principal axes need not be the same, although Neumann's principle requires that they have at least one common axis parallel to the local C_2 symmetry axis. This constraint significantly reduces the number of possible orientations, and we may represent these possibilities on a two-dimensional map.[7] The coordinates of such a map give the particular choice of common axes, and the angle θ through which one set of axes is rotated with respect to the other set about the common axis. Since the Hamiltonian in Eq. (2) is insensitive to the sign of the coordinates, an orientation of, for example, $\hat{x}||\hat{X}$ is equivalent to $\hat{x}||-\hat{X}$. We have calculated the echo modulation curve, Eq. (1), in increments of five degrees in the rotation angle θ. Figure 3 presents a map where for each orientation coordinate a box is drawn whose width is proportional to the minimum mean-square deviation between our data and the calculated curves. Only the first microsecond of data was used in the fitting procedure for Fig. 3. Beyond 1 μsec, the data are dominated by the excited-state hyperfine splittings due to the relative linewidths of ground- and excited-state levels and including these data in the fit considerably reduces the selectivity of the map.

TABLE I. Values for the $^1D_2$ excited-state hyperfine frequencies and nuclear linewidths obtained from the Fourier transform of the data in Fig. 1. The linewidths have been corrected for the effect of the finite truncation interval (Ref. 7).

Resonance	Frequency	Full width at half maximum
ω_1^e	3.72±0.02 MHz	70±20 kHz
ω_2^e	4.79±0.02 MHz	60±20 kHz
ω_{12}^e	8.51±0.02 MHz	30±30 kHz

Figure 4 shows in expanded scale the first three microseconds of (a) our data and (b) the theoretical curve calculated from Eq. (1) using the orientation coordinate giving the best fit to the data (as indicated by an arrow in the lower left of Fig. 3). The curves of Fig. 4, having been multiplied by the factor $\exp(+4\tau/T_2)$, do not include the effect of the overall optical linewidth. The slight rise in the echo peaks of Fig. 4(a) is an artifact in the data due to detector saturation at short pulse separation. This saturation may also be seen in Fig. 1, where the initial envelope decay is somewhat slower than the corresponding decay for the rest of the data. This artifact introduces some uncertainty in the estimate of optical linewidth but seems to have negligible effect on the Fourier transform and overall fit since another data set with smaller overall signal-to-noise ratio, but without the saturation, gives similar results to those presented here.

The map in Fig. 3 shows a high degree of symmetry and concommitant lack of selectivity for

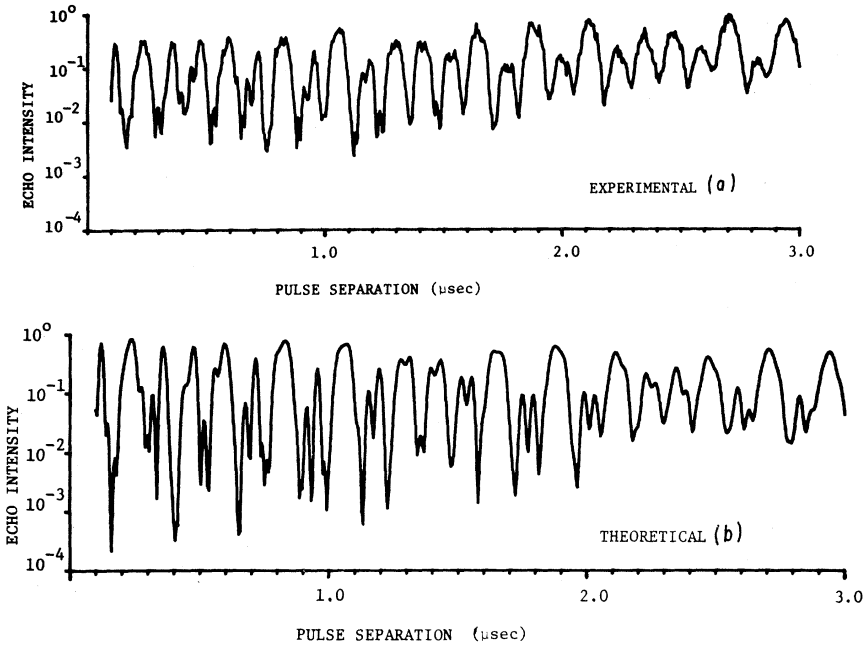

FIG. 4. Comparison of the first three microseconds of data (a) and the theoretical curve (b) for the orientation giving the smallest mean-square deviation.

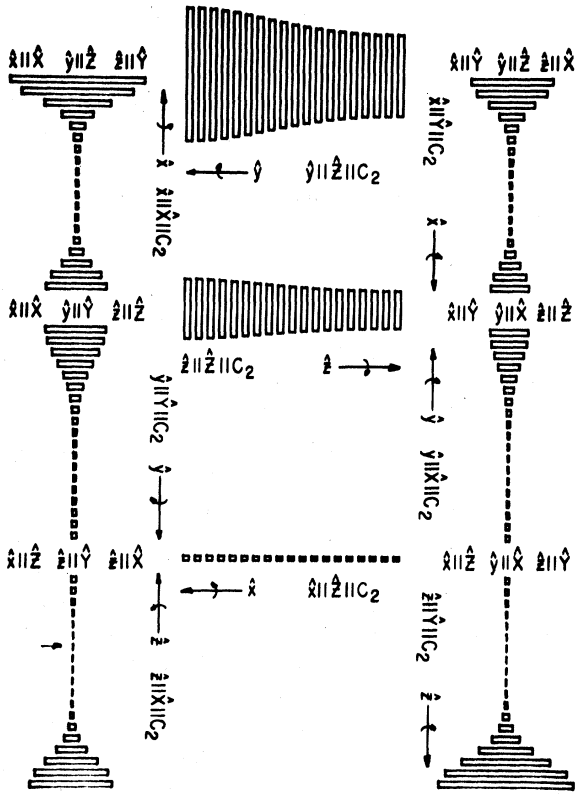

FIG. 5. Map of mean-square deviation between the theoretically calculated data of Fig. 4(b) and the theoretical curve of Eq. (1). Notice the similarity to Fig. 3.

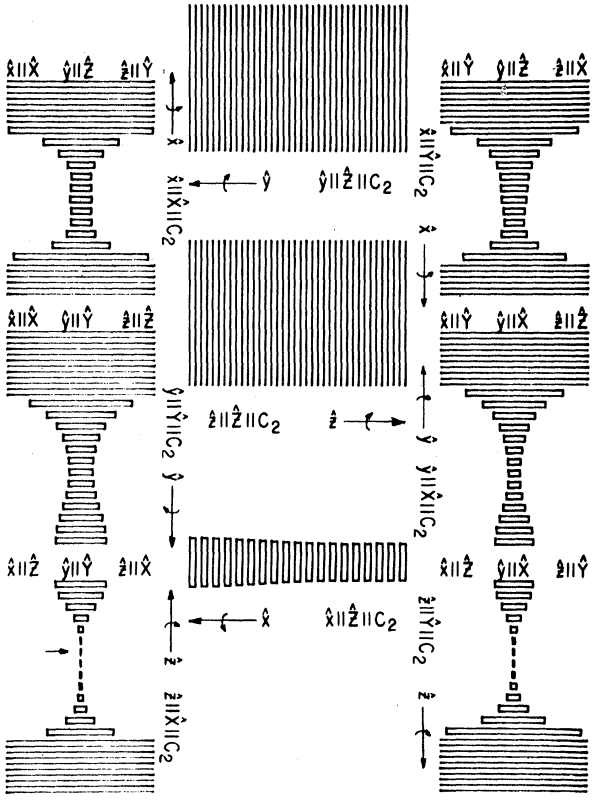

FIG. 6. Map of Fig. 5 with the scale for the box width expanded by a factor of 10.

determining the orientation parameter. To explore the extent to which this symmetry is intrinsic to the form of Eq. (1), we have substituted for the data used to calculate the map of Fig. 3 the values of the theoretical curve corresponding to Fig. 4(b), producing the map shown in Fig. 5. The scale in Fig. 5 was chosen to make the box corresponding to the coordinate with the worst fit in Fig. 5 approximately the same size as the box with the worst fit in Fig. 3. It is apparent that the high degree of symmetry persists. To estimate the extent to which our signal-to-noise ratio would need to improve and so allow us to select one orientation with certainty, we replotted Fig. 5 with the box width scale expanded by a factor of 10, as shown in Fig. 6. It appears that an improvement in the signal-to-noise ratio by a factor of 10 or 20 would have made possible a more definitive statement about the orientation. This improvement will probably come from the use of frequency- and amplitude-stabilized dye lasers. Frequency jitter in particular causes considerable fluctuation in echo intensity, presently averaged by the data-taking system, and such averaging tends to wash out some of the fine details of the modulation pattern. Despite the high symmetry, we can draw a number of conclusions about the relative orientation. All configurations with all axes parallel are ruled out, as are those with the excited-state $\hat{Z}$ axis parallel to C_2. These conclusions are similar to the measurement by Chen *et al.*[7] of the relative orientation of the $^3H_4$ and $^3P_0$ states. Since the g tensor is nearly isotropic in the $^1D_2$ state[10] and absent completely in the $^3P_0$ state, the relative orientation parameter must be primarily determined by the relative orientation of the pure quadrupole tensor with respect to the ground-state hyperfine tensor.

Our photon echo modulation analysis of the $^1D_2$-$^3H_4$ Pr^{3+}:LaF_3 transition hyperfine structure gives a new time-domain measurement of the splittings and linewidths which accords well with previous measurements. We also present new information on the relative orientation of the effective hyperfine Hamiltonians.

One of us (E.W.) wishes to thank Frank Abramopoulis for a useful suggestion concerning the data analysis. This work was supported by the Joint Services Electronics Program (U. S. Army, U. S. Navy, and U. S. Air Force) under Contract No. DAAG29-79-C-0079 and by the National Science Foundation and the Army Research Office under Grant No. NSF-DMR80-06966.

[1]L. E. Erickson, Opt. Commun. 21, 147 (1977).
[2]L. E. Erickson, Phys. Rev. B 16, 4731 (1977).
[3]R. G. DeVoe, A. Wokaun, S. C. Rand, and R. G. Brewer, Phys. Rev. B 23, 3125 (1981).
[4]B. Bleaney, Physica 69, 317 (1973).
[5]R. M. Macfarlane, R. M. Shelby, and R. L. Shoemaker, Phys. Rev. Lett. 43, 1726 (1979).
[6]K. Chiang, E. A. Whittaker, and S. R. Hartmann, Phys. Rev. B 23, 6142 (1981).
[7]Y. C. Chen, K. Chiang, and S. R. Hartmann, Phys. Rev. B 21, 40 (1980).
[8]Y. C. Chen, K. Chiang, and S. R. Hartmann, Opt. Commun. 29, 269 (1979). The artifact occurs because a three-pulse stimulated echo, formed by two excitation pulses of one laser shot and the second excitation pulse of the succeeding shot, occurs simultaneous with the ordinary echo signal. This effect was not compensated for in the experiment of Ref. 7 and may have distorted their result somewhat.
[9]R. G. DeVoe, A. Szabo, S. C. Rand, and R. G. Brewer, Phys. Rev. Lett. 42, 1560 (1979).
[10]R. M. Macfarlane and R. M. Shelby, Opt. Lett. 6, 96 (1981).